*Proceedings of the Korean Nuclear Society Spring Meeting*
*Seoul, Korea, May 1998*

# Theoretical Prediction Method of Subcooled Flow Boiling CHF

Young Min Kwon* and Soon Heung Chang
* Korea Atomic Energy Research Institute
Korea Advanced Institute of Science and Technology

**Abstract**

A theoretical critical heat flux (CHF) model, based on lateral bubble coalescence on the heated wall, is proposed to predict the subcooled flow boiling CHF in a uniformly heated vertical tube. The model is based on the concept that a single layer of bubbles contacted to the heated wall prevents a bulk liquid from reaching the wall at near CHF condition. Comparisons between the model predictions and experimental data result in satisfactory agreement within less than 9.73 % root-mean-square error by the appropriate choice of the critical void fraction in the bubbly layer. The present model shows comparable performance with the CHF look-up table of Groeneveld et al..

## 1. INTRODUCTION

Over the last several decades, numerous mechanistic models have been proposed to describe a critical heat flux (CHF) in subcooled flow boiling, however, no satisfactory model can yet explain the trigger mechanism responsible for the onset of CHF. Most of the mechanistic CHF model is based on hypothetical assumptions regarding flow structure of the near-wall when heat flux approaches CHF condition. Prediction accuracy is dependent on the limited applicability of various constitutive relations employed within them as well as empirical constants.

According to recent reviews about the analytical modeling of CHF (Weisman, 1992; Katto, 1994; Celata, 1997), among many existing models available today, only near wall bubble crowding (Weisman and co-workers, 1983; 1985; 1988) and liquid sublayer dryout (Lee-Mudawar, 1988; Katto, 1992; Celata et al., 1994a) models have widely attracted attention for the prediction of the CHF in the moderate and highly subcooled conditions. However, comparative analyses performed by Iwamura et al. (1992), Celata et al. (1994b), and Bricard and Souyri (1995) show that the predictive capabilities of all the present theoretical CHF models are not enough to apply them to new system designs.

Chang and Lee (1989) presented a mechanistic model of CHF based on the bubble crowding mechanism, where the CHF formula was derived from mass, energy and momentum balance equations. Recently, Lee et al. (1997) modified the Chang and Lee's model according to Bricard and Souyri's (1995) comments. They fixed mistakes included in the original model without imposing the stagnated bubbly layer. In the present study, a new CHF model is developoed, where the bubbly layer is represented as a single layer of bubbles contacted to the heated wall. The model is validated on the experimental CHF data of water in uniformly heated tubes and compared with the prediction capabilities of the CHF loo-kup table of Groeneveld et al. (1996).

## 2. PHYSICAL SYSTEM AND BASIC ASSUMPTIONS

Tong and Hewitt (1972) have described the CHF as a boiling crisis arising from the spreading of a dry patch

following microlayer evaporation under a bubble, and a coalescence of adjacent bubbles. If the characteristic is postulated, the bubbles are discrete and attached to a heated wall at the condition of CHF. A hypothetical flow structure considered in this study is shown in Fig.1. In the outer annular layer of the round tube, independent bubbles compact on the wall just prior to agglomeration and in the middle of the tube is a mixture core consisting of liquid and bubbles.

Earlier work by Beattie (1980) has shown that wall bubbles act as a surface roughness equivalent to bubble size. Under such conditions, friction factor can be described by the same form of equation as that used for single-phase flow in roughned tubes. Although Beattie considered flow remote from the CHF, it can be supposed that bubbles in the boiling crisis region behave similarly. Therefore, attached bubbles are considered as increasing wall roughness of the tube and result in increasing the value of friction factor.

Gunther (1951) and Kirby et al. (1967) observed that the two-phase layer of local vapor film in subcooled flow boiling was one bubble thick, while Mattson et al. (1973) observed it was an order of magnitude thicker than the maximum diameter. The bubbly layer thickness is a characteristic parameter in the bubble crowding model, it was assumed to be 2.5 times of bubble diameter in Weisman and Pei model (1983) and 1.7 times in Chang-Lee model (1989). The thickness was determined empirically by fitting the CHF model to a large number of CHF experimental data.

The effective thickness of bubbly layer is considered as a single bubble diameter in the present work. It is hypothesized that only the near-wall bubbles play the effective physical barrier of the heat transfer from the wall and liquid supply from the core region. As heat flux approaches to the CHF, active nucleation site density increases. When the number of bubbles surrounding one bubble becomes numerous, bubbles overlap due to lateral coalescence and a bubbly layer may be made. For forced flow condition, above the coalescent plane shown in Fig.2, detached vapor bubbles migrated from upstream may block the liquid between surrounding bubbles attached to the wall, which accelerate to coalesce bubbles into a large vapor clot. Consequently, a certain amount of liquid will be trapped underneath the plane of coalescence of bubbles.

In this situation, the increased bubble concentration possibly combined with interfacial instability may restrict the feed of liquid to the thin liquid film under the bubbly layer. It is postulated that CHF occurs at the instant the liquid in the bubbly layer dries out without liquid supply from outwards when mass flux from core, $G_{cb}$, is equal to outward one to core, $G_{bc}$, at the outer edge of the bubbly layer. At this situation, when a large merged vapor clot is torn off from the wall, the flow structure near the wall becomes similar to that of the sublayer dryout model.

The critical void fraction, $\alpha_b$, is defined as a volume fraction of steam in the bubbly layer at which CHF occurs. Because experimental information of $\alpha_b$ is not available until now, simple bubble configurations, as examples, are shown in Fig. 2. Because the critical void fraction is a complex function of size and population density of bubbles, a sensitivity of the critical void fraction on the CHF predictions is conducted. The lower limit of 0.524 is based on the Fig. 2-(a), and 0.605 is based on the Fig. 2-(b). Figure 2-(c) is the case where an overlap between surrounding bubbles occurs, resulting in higher wall void fraction. The upper limit of 0.90 is selected arbitrarily. It is worth noting that values of 0.82 and 0.75 were utilized by Weisman and Pei, and Chang and Lee in their CHF models, respectively. For a more accurate prediction of critical void fraction, further investigation on the distribution of active sites within the influence of a bubble is required.

## 3. PHENOMENOLOGICAL MODEL

In the present study, one-dimensional steady state subcooled flow boiling in a tube is analyzed with the

effects of two-phase flow model and constitutive equations. Considering a bubbly layer control volume as shown in Fig. 1, the total flow rate from core to bubbly layer must be equal to the total flow rate from bubbly to core plus the axial flow in and out of the bubbly layer control volume. Chang and Lee obtained a CHF equation related to a boiling heat flux, $q''_b$, from mass and energy balances over the bubbly layer as

$$q''_{CHF} = \frac{q''_b}{F_q} = \frac{q''_b(h_b - h_c)}{h_{fg}(x_b - x_c)} = G^*(h_b - h_c)\frac{\xi_i}{\xi_w}, \tag{1}$$

where the factor, $F_q$, represents the fraction of the heat flux producing vapor that enters the core region. The qualities in eq. (1) are actual flow qualities based on a homogeneous nonequilibrium condition. The value of $x_b$ (see Nomenclature) is the quality corresponding to the critical void fraction, $\alpha_b$, which is discussed later. Flow enthalpies in core and bubbly layer regions are defined as, respectively

$$h_c = h_l(1-\alpha_c) + h_g\alpha_c, \qquad h_b = h_f(1-\alpha_b) + h_g\alpha_b \tag{2}$$

Based on one-dimensional momentum equation of separated flow model (Lahey and Moody, 1993), we obtain the transverse interchange of mass flux at the bubbly-core interface as

$$G^* = \left[-(\rho_c - \rho_b)g + \frac{\tau_w\xi_w}{A(1-\beta_c)} + \Phi_{acc}\right]\frac{A\beta_c(1-\beta_c)}{(\overline{U}_c - \overline{U}_b)\xi_i}. \tag{3}$$

Equation (3) is derived based on the following assumptions. As CHF condition, the transverse mass transport rate at the interface is limited, i.e., $G^* = G_{bc} = G_{cb}$. Because the heated surface is considered to be contact to discrete bubbles in the bubbly layer, the bubbly layer is assumed to transmit to the heated wall the shear force exerted by the liquid just outside the bubbly layer. The acceleration term $\Phi_{acc}$ in eq. (3) is defined as

$$\Phi_{acc} = \frac{1}{A_b}\frac{d}{dz}\left(\rho_b\overline{U}_b^{\,2}A_b\right) - \frac{1}{A_c}\frac{d}{dz}\left(\rho_c\overline{U}_c^{\,2}A_c\right). \tag{4}$$

Chang and Lee have shown that the acceleration term was negligibly small with respect to the radial mixing flow effect. Theoretically, $\Phi_{acc}$ is able to be calculated using two-phase flow identities, but that brings in more complexity in the CHF calculation. The acceleration influence is neglected in the present study for simplicity.

The wall shear stress is calculated as $\tau_w = 0.5f\rho_c\overline{U}_c^{\,2}$. In the Chang and Lee model, Nedderman and Shearer's (1964) friction factor model was used with the idea that the bubble layer might behave like the regular sand roughness used by Nikuradse in his experiments. In the present work, the bubbly layer probably acts more like the random roughness found in commercial tubes and piping, because the bubbles are growing and collapsing and also sliding along the wall. The turbulent friction factor, $f$, is calculated using the Colebrook and White equation with a two-phase Reynolds number to account for the variation of the fluid viscosity near the heated wall

$$\frac{1}{\sqrt{f}} = 3.48 - 4\log\left(\frac{D_b}{D} + \frac{9.35}{\mathrm{Re}_{2\phi}\sqrt{f}}\right), \qquad \mathrm{Re}_{2\phi} = \frac{GD}{\mu_{2\phi}} \tag{5}$$

where the surface roughness is assumed to be equivalent to $\varepsilon/D = D_b/2D$. It is consistent with the assumption of Staub's (1968) physical model of bubble departure diameter where he considered a drag force works on the bubbly layer, not on a single bubble.

The average velocity of the bubbly layer, $\overline{U}_b$, is determined by taking it as half the velocity of the core at the outer edge of the bubbly layer, because the velocity profile in the bubbly layer is near linear due to its very thin

thickness.

$$\overline{U}_b = 0.5U_c (at\ y = D_b), \qquad \overline{U}_c = \frac{G\zeta_c}{\rho_c \beta_c} \tag{6}$$

where $y$ is a distance form the wall in the radial direction. The universal logarithmic velocity profile for a single phase turbulent flow proposed by Karman is assumed to be valid in the turbulent core region as

$$U^+ = Y^+ \qquad 0 \le Y^+ < 5, \tag{7}$$

$$U^+ = 5\ln Y^+ - 3.05 \qquad 5 \le Y^+ < 30, \tag{8}$$

$$U^+ = 2.5\ln Y^+ + 5.5 \qquad 30 \le Y^+, \tag{9}$$

$$U^+ = \frac{U_c}{U^*}, \quad Y^+ = \frac{\rho_c U^* y}{\mu_{2\phi}}, \quad U^* = \sqrt{\frac{\tau_w}{\rho_c}}, \quad \tau_w = \frac{fG^2}{8\rho_c} \tag{10}$$

Because the flows of core and bubbly layer regions are assumed to be homogeneous, the quantities used in above equations are defined as

$$\rho_c = \rho_l(1-\alpha_c) + \rho_g \alpha_c, \qquad \rho_b = \rho_f(1-\alpha_b) + \rho_g \alpha_b, \tag{11}$$

$$\mu_{2\phi} = \mu_f(1-\alpha_g)(1+2.5\alpha_g) + \mu_g \alpha_g, \qquad \alpha_g = \beta_c \alpha_c + (1-\beta_c)\alpha_b, \tag{12}$$

$$\beta_c = \frac{A_c}{A} = \frac{(D-2D_b)^2}{D^2}, \qquad \zeta_c = 1 - \frac{\overline{U}_b \rho_b (1-\beta_c)}{G}, \tag{13}$$

where $\beta_c$ and $\zeta_c$ denote the fraction of cross-section occupied by core and the fraction of mass flux in core, respectively. The average viscosity of core region, $\mu_{2\phi}$, is evaluated by Beattie and Whalley (1982). The Effect of pressure variation along the tube is neglected and calculation is performed with the assumption that pressure at each point equals the exit pressure.

In order to achieve closure of the mass, energy and momentum balance equations for CHF model, several additional constitutive relations are required. For an accurate prediction of actual flow quality and enthalpy at the location of CHF occurrence, the void fraction profile in the subcooled flow boiling should be determined appropriately. For this purpose, the Levy (1967) model which balances buoyancy and drag forces against surface tension force is employed. The detached bubble diameter, neglecting buoyancy force at high velocity region, is evaluated by

$$D_b = 0.015\sqrt{\frac{8\sigma D\overline{\rho}}{f' G^2}}, \tag{14}$$

where $\overline{\rho}$ and f' are average density at the tube exit and Darcy-Weisbach friction factor, respectively, adopted in Levy's model. The friction factor $f'$ compares well with the $f$ of eq. (5) in the fully turbulent flow regime. The flow quality can be evaluated by both profile-fit and mechanistic approaches according to Lahey and Moody (1993). Because little difference in the CHF predictions appears when both approaches are applied to the present CHF model, the simple profile-fit model of Saha and Zuber (1974) is utilized. The relationship between the true flow quality and the thermodynamic equilibrium quality is predicted by

$$x = \frac{x_e - x_d \exp(x_e / x_d - 1)}{1 - x_d \exp(x_e / x_d - 1)}, \tag{15}$$

where $x_d$ and $x_e$ are thermodynamic qualities at the onset of a significant void (OSV) point and tube exit, respectively. According to the critical review of predictive models for the OSV performed by Lee et al. (1992), the Levy model is the best one among the analytical models. Once the flow quality at the tube exit is determined using eq. (25), the subcooled void fraction is calculated using Chexal-Lellouche (1991) model that successfully covers a wide range of pressure, flow, and void fraction.

An insight into the relationship between CHF mechanism and the various parameters appearing in the above equations can be drawn. It is indicated that local friction factor and local flow quality as well as mass flux, tube geometry, choice of fluid, and system pressure are major parameters. This implies that both hydrodynamic and thermal factors play a role in the onset of CHF in the present model as pointed out by Tong and Hewitt (1972). In the present model, only one empirical parameter of $\alpha_b$ is employed by fitting to experimental CHF data, however, three empirical constants were used in Weisman and Pei model and two constants in Chang and Lee model. The basis of the critical void fraction may be derived from the theoretical investigation with the aid of experimental observation in the future.

## 4. COMPARISON WITH EXPERIMENTAL DATA

The results of comparison against experimental data are quantitatively evaluated by the CHFR, defined as the predicted CHF to the measured CHF. A total of 905 water CHF data points for uniformly heated vertical round tubes are obtained from KAIST CHF data base (Chang et al., 1996). The parametric ranges are diameters from 2 mm to 37.5 mm, lengths from 0.035 m to 4 m, mass fluxes from 500 to 10058 kg/m$^2$s, pressures from 5 to 20 MPa, outlet qualities from –0.5 to 0.001, and critical heat fluxes from 761 to 24800 kW/m$^2$.

The effects of $\alpha_b$ on predictions of the CHF are investigated by varying its value from 0.524 to 9.0, as previously discussed in section 2. The best constant value of $\alpha_b$, resulting in an average CHFR of 1.0 while minimizing a root-mean-square (RMS) error of CHFR, is found to be 0.70, which predicts about all data points within a RMS of 9.73 %. Table 1 summarizes the prediction results of the present model. Here N stands for the number of data points predicted successfully by the present CHF model, $\mu$ for the average value of the CHFR and $\sigma$ and *RMS* stand for the standard deviation and the root-mean-square error. Fig.3 shows the visual comparison of the predicted and measured CHF and most of the experiment data are successfully predicted within 20% error bounds. The percentage of data points calculated with the corresponding error band (±%) is presented in Fig. 4. The prediction accuracy increases as $\alpha_b$ increases up to 0.7, while it deteriorates after 0.7. For conditions where the $\alpha_b$ is higher than 0.9, the number of CHF data points predicted successfully and their accuracy are rapidly reduced.

The dependence of the prediction accuracy on major parameters are presented in Fig. 5 through Fig. 10. Comparison of theoretical predictions from the present CHF model with experimental data does not seem to exhibit systematic deviations which could be attributed to a certain system parameter, such as thermal hydraulic conditions (P, G, $\alpha$, $\Delta h_i$) and geometric parameters (D and L/D). For comparing with the present model, the predictions using CHF look-up table of Groeneveld (1996) are performed based on the so-called heat balance method (HBM). Because the look-up table has its applicable ranges, 882 data points are used for comparison. For tubes of diameter other than 8 mm, the diameter correction equation suggested by the table authors is used. The

average value of the CHFR is 1.017. The standard deviation and RMS are 10.62 % and 10.75 %, respectively. Figure 11 shows the comparisons of 882 data points with the CHF look-up table. The percentage of data points calculated with the corresponding error band (±%) for the look-up table including the present one is presented in Fig. 4.

It is suggested here that the lateral coalescence can take place if the void fraction of bubbly layer reaches a certain critical value of 0.7 when heat flux approaches CHF. The effect of coalescence will eventually result in the formation of large vapor clots or bubble crowding under which liquid is trapped. We have ignored the statistical variations in bubble size and population density which are important for the bubble coalescence on the heated wall. Because the complex phenomena of bubble agglomeration can not be represented by the present analytical frame of balance equations, the process of CHF after formation of a vapor clot is to be represented by different view point, such as sublayer dryout models.

## 5. CONCLUSION

A theoretical model based on lateral bubbles coalescence on the heated wall has been developed to predict the CHF during subcooled flow boiling in a uniformly heated vertical tube. Comparison of the current model predictions to the experimental CHF data shows that the predictions are nearly as accurate as the CHF look-up table of Groneveld (1996). With adjustment of only one empirical constant for the critical void fraction, a relatively good prediction has been performed within ±20% error bounds. The overall mean ratio of predicted to measured CHF values is 1.004 with a standard deviation of 9.72 % and a RMS error of 9.73 % against 905 water CHF data points. It can be suggested that the dominant mechanism controlling CHF in subcooled flow boiling is properly represented with the present model. It is suggested that refinement of this model should be pursued in the future to improve the critical void fraction in the bubbly layer. Furthermore, improvement in the current model can readily be made if better constitutive laws are used for the various phenomena governing nucleation and bubble departure from the wall.

**Nomenclature**

A cross-section area,
D tube diameter,
$D_b$ detached bubble diameter,
G mass flux,
$G^*$ limited mixing mass flux,
f,f' skin friction factor,
g acceleration due to gravity,
h enthalpy,
$h_{fg}$ vaporization latent enthalpy
P pressure,
q'' heat flux,
U mean velocity,
x flow quality,
y distance in radial direction,
$\alpha$ void fraction,
$\beta$ fraction of cross-section area
$\rho$ density,
$\mu$ viscosity,
$\sigma$ surface tension,
$\tau$ shear stress,
$\zeta$ fraction of mass flux,
$\xi$ perimeter,

subscripts
$2\phi$ two-phase mixture flow,
b bubbly layer,
bc from bubbly layer to core,
c core,
cb from core to bubbly layer,
CHF at CHF condition,
d bubble detached position,
e equilibrium condition,
f saturated liquid,
g vapor phase or overall,
l subcooled liquid,
w at the heated wall.

**References**


1. D. R. H. Beattie, NUREG/CP-0014, p.1343 (1980)
2. D. R. Beattie and P. B. Whalley, Int. J. Multiphase Flow, Vol. 8, pp. 83-87 (1982)
3. P. Bricard and A. Souyri, Two-phase flow modeling and experimentation, Edizioni ETS, pp.843-851 (1995)
4. G. P. Celata et al., Int. J. Heat Mass Transfer, Vol. 37, suppl.1, pp. 347-360 (1994a)
5. G. P. Celata et al., Int. J. Heat Mass Transfer, Vol. 37, pp. 237-255 (1994b)
6. G. P. Celata, Convective flow and pool boiling conference, Kloster Irsee, Germany, May (1997)

$$x = \frac{x_e - x_d \exp(x_e / x_d - 1)}{1 - x_d \exp(x_e / x_d - 1)}, \tag{15}$$

where $x_d$ and $x_e$ are thermodynamic qualities at the onset of a significant void (OSV) point and tube exit, respectively. According to the critical review of predictive models for the OSV performed by Lee et al. (1992), the Levy model is the best one among the analytical models. Once the flow quality at the tube exit is determined using eq. (25), the subcooled void fraction is calculated using Chexal-Lellouche (1991) model that successfully covers a wide range of pressure, flow, and void fraction.

An insight into the relationship between CHF mechanism and the various parameters appearing in the above equations can be drawn. It is indicated that local friction factor and local flow quality as well as mass flux, tube geometry, choice of fluid, and system pressure are major parameters. This implies that both hydrodynamic and thermal factors play a role in the onset of CHF in the present model as pointed out by Tong and Hewitt (1972). In the present model, only one empirical parameter of $\alpha_b$ is employed by fitting to experimental CHF data, however, three empirical constants were used in Weisman and Pei model and two constants in Chang and Lee model. The basis of the critical void fraction may be derived from the theoretical investigation with the aid of experimental observation in the future.

## 4. COMPARISON WITH EXPERIMENTAL DATA

The results of comparison against experimental data are quantitatively evaluated by the CHFR, defined as the predicted CHF to the measured CHF. A total of 905 water CHF data points for uniformly heated vertical round tubes are obtained from KAIST CHF data base (Chang et al., 1996). The parametric ranges are diameters from 2 mm to 37.5 mm, lengths from 0.035 m to 4 m, mass fluxes from 500 to 10058 kg/m$^2$s, pressures from 5 to 20 MPa, outlet qualities from –0.5 to 0.001, and critical heat fluxes from 761 to 24800 kW/m$^2$.

The effects of $\alpha_b$ on predictions of the CHF are investigated by varying its value from 0.524 to 9.0, as previously discussed in section 2. The best constant value of $\alpha_b$, resulting in an average CHFR of 1.0 while minimizing a root-mean-square (RMS) error of CHFR, is found to be 0.70, which predicts about all data points within a RMS of 9.73 %. Table 1 summarizes the prediction results of the present model. Here N stands for the number of data points predicted successfully by the present CHF model, $\mu$ for the average value of the CHFR and $\sigma$ and *RMS* stand for the standard deviation and the root-mean-square error. Fig.3 shows the visual comparison of the predicted and measured CHF and most of the experiment data are successfully predicted within 20% error bounds. The percentage of data points calculated with the corresponding error band (±%) is presented in Fig. 4. The prediction accuracy increases as $\alpha_b$ increases up to 0.7, while it deteriorates after 0.7. For conditions where the $\alpha_b$ is higher than 0.9, the number of CHF data points predicted successfully and their accuracy are rapidly reduced.

The dependence of the prediction accuracy on major parameters are presented in Fig. 5 through Fig. 10. Comparison of theoretical predictions from the present CHF model with experimental data does not seem to exhibit systematic deviations which could be attributed to a certain system parameter, such as thermal hydraulic conditions (P, G, $\alpha$, $\Delta h_i$) and geometric parameters (D and L/D). For comparing with the present model, the predictions using CHF look-up table of Groeneveld (1996) are performed based on the so-called heat balance method (HBM). Because the look-up table has its applicable ranges, 882 data points are used for comparison. For tubes of diameter other than 8 mm, the diameter correction equation suggested by the table authors is used. The

average value of the CHFR is 1.017. The standard deviation and RMS are 10.62 % and 10.75 %, respectively. Figure 11 shows the comparisons of 882 data points with the CHF look-up table. The percentage of data points calculated with the corresponding error band (±%) for the look-up table including the present one is presented in Fig. 4.

It is suggested here that the lateral coalescence can take place if the void fraction of bubbly layer reaches a certain critical value of 0.7 when heat flux approaches CHF. The effect of coalescence will eventually result in the formation of large vapor clots or bubble crowding under which liquid is trapped. We have ignored the statistical variations in bubble size and population density which are important for the bubble coalescence on the heated wall. Because the complex phenomena of bubble agglomeration can not be represented by the present analytical frame of balance equations, the process of CHF after formation of a vapor clot is to be represented by different view point, such as sublayer dryout models.

## 5. CONCLUSION

A theoretical model based on lateral bubbles coalescence on the heated wall has been developed to predict the CHF during subcooled flow boiling in a uniformly heated vertical tube. Comparison of the current model predictions to the experimental CHF data shows that the predictions are nearly as accurate as the CHF look-up table of Groneveld (1996). With adjustment of only one empirical constant for the critical void fraction, a relatively good prediction has been performed within ±20% error bounds. The overall mean ratio of predicted to measured CHF values is 1.004 with a standard deviation of 9.72 % and a RMS error of 9.73 % against 905 water CHF data points. It can be suggested that the dominant mechanism controlling CHF in subcooled flow boiling is properly represented with the present model. It is suggested that refinement of this model should be pursued in the future to improve the critical void fraction in the bubbly layer. Furthermore, improvement in the current model can readily be made if better constitutive laws are used for the various phenomena governing nucleation and bubble departure from the wall.

**Nomenclature**

| | |
|---|---|
| A | cross-section area, |
| D | tube diameter, |
| $D_b$ | detached bubble diameter, |
| G | mass flux, |
| $G^*$ | limited mixing mass flux, |
| f,f' | skin friction factor, |
| g | acceleration due to gravity, |
| h | enthalpy, |
| $h_{fg}$ | vaporization latent enthalpy |
| P | pressure, |
| q'' | heat flux, |
| U | mean velocity, |
| x | flow quality, |
| y | distance in radial direction, |
| $\alpha$ | void fraction, |
| $\beta$ | fraction of cross-section area |
| $\rho$ | density, |
| $\mu$ | viscosity, |
| $\sigma$ | surface tension, |
| $\tau$ | shear stress, |
| $\zeta$ | fraction of mass flux, |
| $\xi$ | perimeter, |

subscripts

| | |
|---|---|
| $2\phi$ | two-phase mixture flow, |
| b | bubbly layer, |
| bc | from bubbly layer to core, |
| c | core, |
| cb | from core to bubbly layer, |
| CHF | at CHF condition, |
| d | bubble detached position, |
| e | equilibrium condition, |
| f | saturated liquid, |
| g | vapor phase or overall, |
| l | subcooled liquid, |
| w | at the heated wall. |

**References**


1. D. R. H. Beattie, NUREG/CP-0014, p.1343 (1980)
2. D. R. Beattie and P. B. Whalley, Int. J. Multiphase Flow, Vol. 8, pp. 83-87 (1982)
3. P. Bricard and A. Souyri, Two-phase flow modeling and experimentation, Edizioni ETS, pp.843-851 (1995)
4. G. P. Celata et al., Int. J. Heat Mass Transfer, Vol. 37, suppl.1, pp. 347-360 (1994a)
5. G. P. Celata et al., Int. J. Heat Mass Transfer, Vol. 37, pp. 237-255 (1994b)
6. G. P. Celata, Convective flow and pool boiling conference, Kloster Irsee, Germany, May (1997)

7. S. H. Chang and K. W. Lee, Nucl. Eng. Des., Vol. 113, pp. 35-50 (1989)
8. S. H. Chang et al., The KAIST CHF Data Bank (Rev. 3), KAIST-NUSCOL-9601 (1996)
9. B. Chexal, J. Horowitz, and G. S. Lellouche, Nucl. Eng. Des., 126, pp. 71-88 (1991)
10. D. C. Groeneveld et al., Nucl. Eng. Des., Vol. 163, pp.1-23 (1996)
11. F. C. Gunther, TRANS. ASME , Vol.73, pp. 115-121 (1951)
12. T. Iwamura et al., JAERI-M 92-033, JAERI (1992)
13. Y. Katto, Int. J. Heat Mass Transfer, Vol. 35, No.5, pp. 1115-1123 (1992)
14. Y. Katto, Int. J. Multiphase Flow, Vol. 20, pp. 53-90 (1994)
15. G. J. Kirby, R. Staniforth, and L. H. Kinneir, AEEW-R-506, UKAEA, Winfrith (1967)
16. R. T. Lahey, Jr. and F. J. Moody, The Thermal-Hydraulics of a Boiling Water Nuclear Reactor, American Nuclear Society, second ed., La Grange Park, Illinois (1993)
17. C. H. Lee and I. Mudawar, Int. J. Multiphase Flow, Vol. 14, pp. 714-728, (1988)
18. K. W. Lee et al., 5th NUTHOS, Beijing, China (1997)
19. S. C. Lee, H. Dorra and S. G. Bankoff, HTD-Vol.217, ASME, pp. 33-39 (1992)
20. S. Levy, Int. J. Heat Mass Transfer, Vol. 10, pp. 951-965 (1967)
21. R. J. Mattson, F. G. Hammitt, and L. S. Tong, ASME Paper 73-HT-39 (1973)
22. R. M. Nedderman ans C. J. Shearer, Chem. Eng. Sci., Vol.19, pp. 423-428 (1964)
23. F. W. Staub, Vol.90, pp. 151-157 (1968)
24. L. S. Tong and G. F. Hewitt, ASME Paper 72-HT-54 (1972)
25. L. S. Tong and J. Weisman, Thermal Analysis of Pressurized Water Reactors, ANS, third ed. (1996)
26. J. Weisman and B. S. Pei, Int. J. Heat Mass Transfer, Vol. 26, pp. 1463-1477 (1983)
27. J. Weisman and S. Ileslamlou, Fusion Tech., Vol.13, pp. 654-659 (1988)
28. J. Weisman, Nucl. Tech., Vol. 99, pp. 1-21 (1992)

Table 1. Comparison of predictions of the present model and the CHF look-up table of Groeneveld et al.(1996)

| Prediction Methods | Number of Data Points (N)* | Average Mean value ($\mu$) | RMS error | Standard Deviation ($\sigma$) |
|---|---|---|---|---|
| Current model | | | | |
| $\alpha_b$=0.524 | 901 | 0.888 | 14.78 | 9.53 |
| $\alpha_b$=0.6 | 904 | 0.928 | 11.85 | 9.42 |
| $\alpha_b$=0.7 | 905 | 1.004 | 9.73 | 9.72 |
| $\alpha_b$=0.82 | 905 | 1.158 | 19.78 | 11.97 |
| $\alpha_b$=0.9 | 895 | 1.344 | 38.40 | 17.07 |
| CHF look-up table | 882 | 1.017 | 10.75 | 10.65 |

* N means the number of predictable cases among 905 experimental data points.

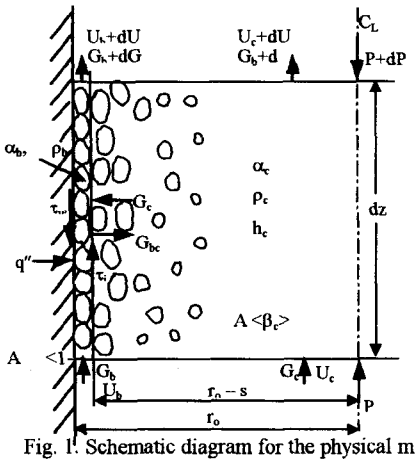


Fig. 1. Schematic diagram for the physical model

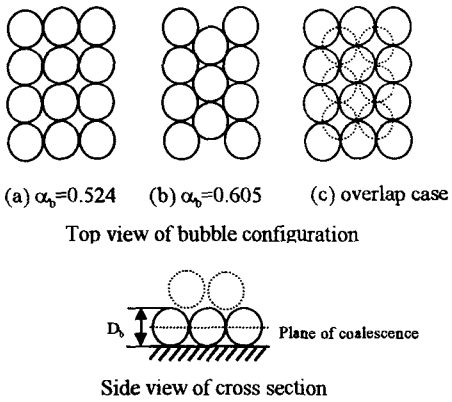


Fig. 2. Configuration of bubbles on the heated wall

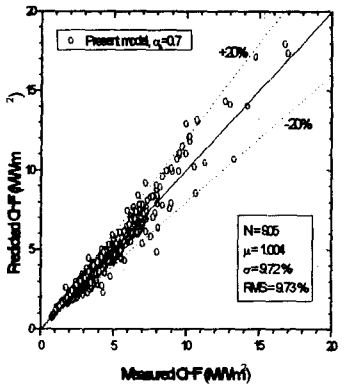


Fig. 3. CHF predictions by the present model ($\alpha_b$ = 0.7)

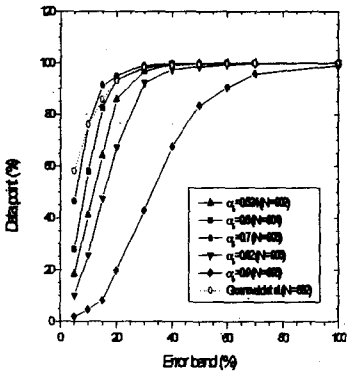


Fig. 4. Percentage of data points predicted within error band

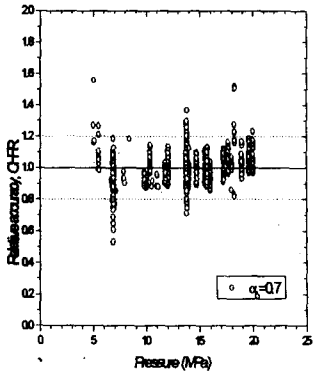


Fig. 5. CHFR vs pressure

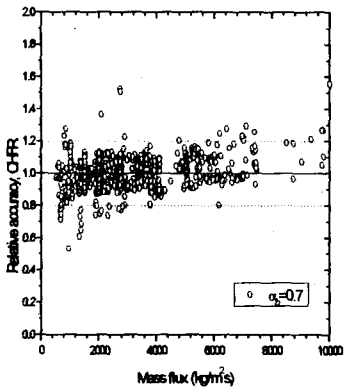


Fig. 6. CHFR vs mass flux

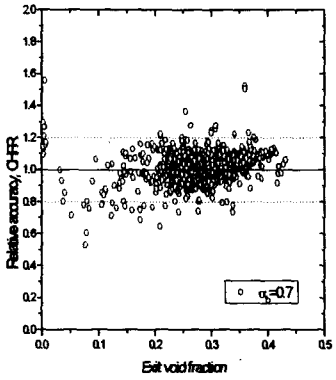


Fig. 7. CHFR vs exit void fraction

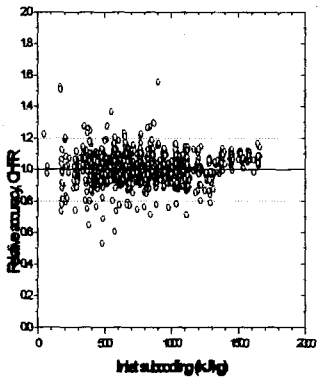


Fig. 8. CHFR vs inlet subcooling

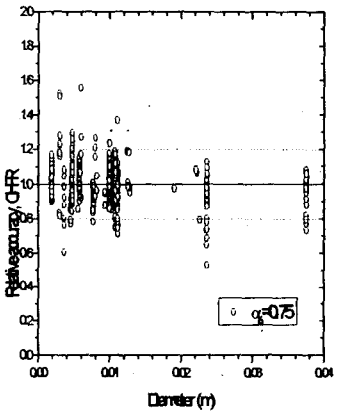


Fig. 9. CHFR vs tube diameter

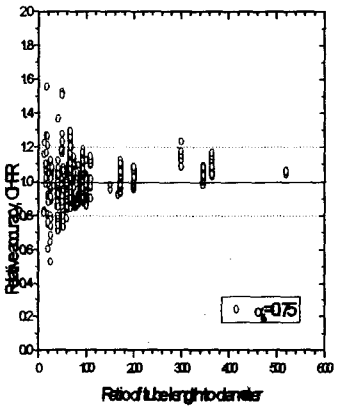


Fig. 10. CHFR vs ratio of tube Length to diameter

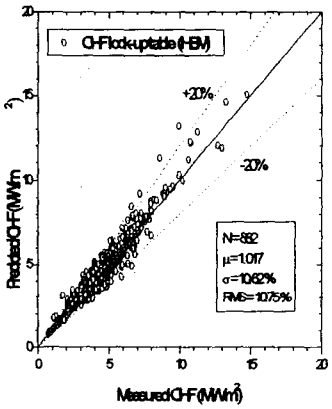


Fig. 11. CHF predictions by the look-up table of Groeneveld et al.